Muscular Forces from Static Optimization

by

Sofia Heintz

April 2006
Technical Reports from
Royal Institute of Technology
KTH Mechanics
SE-100 44 Stockholm, Sweden

Abstract

At every joint there is a redundant set of muscle activated during movement or loading of the system. Optimization techniques are needed to evaluate individual forces in every muscle. The objective in this thesis was to use static optimization techniques to calculate individual muscle forces in the human extremities.

A cost function based on a performance criterion of the involved muscular forces was set to be minimized together with constraints on the muscle forces, restraining negative and excessive values. Load-sharing, load capacity and optimal forces of a system can be evaluated, based on a description of the muscle architectural properties, such as moment arm, physiological cross-sectional area, and peak isometric force.

The upper and lower extremities were modelled in two separate studies. The upper extremity was modelled as a two link-segment with fixed configurations. Load-sharing properties in a simplified model were analyzed. In a more complex model of the elbow and shoulder joint system of muscular forces, the overall total loading capacity was evaluated.

A lower limb model was then used and optimal forces during gait were evaluated. Gait analysis was performed with simultaneous electromyography (EMG). Gait kinematics and kinetics were used in the static optimization to evaluate of optimal individual muscle forces. EMG recordings measure muscle activation. The raw EMG data was processed and a linear envelope of the signal was used to view the activation profile. A method described as the EMG-to-force method which scales and transforms subject specific EMG data is used to compare the evaluated optimal forces.

Reasonably good correlation between calculated muscle forces from static optimization and EMG profiles was shown. Also, the possibility to view load-sharing properties of a musculoskeletal system demonstrate a promising complement to traditional motion analysis techniques. However, validation of the accurate muscular forces are needed but not possible.

Future work is focused on adding more accurate settings in the muscle architectural properties such as moment arms and physiological cross-sectional areas. Further perspectives with this mathematic modelling technique include analyzing pathological movement, such as cerebral palsy and rheumatoid arthritis where muscular weakness, pain and joint deformities are common. In these, better understanding of muscular action and function are needed for better treatment.

Preface

”Biomechanics sounds like fun!” I thought when Prof. Anders Eriksson suggested PhD-studies in the subject. ”Interesting, challenging and hard work!” are the words I use today, realizing the distance between civil engineering and biomechanical engineering.

The work finally ended in this licenciate thesis which is based on two articles which were made possible by support from supervisors, colleagues, friends and family. I give my sincere gratitude to:

Prof. Anders Eriksson my main supervisor, who gave me the opportunity to accomplish this work in this, for me relative new, area. Also, for his guidance and sharing of his knowledge.

Dr. Lanie Gutierrez-Farewik my co-supervisor, for making me believe in myself with her positive attitude. Your knowledge, support and guidance are essential in the accomplishment of this thesis.

Dr. Gunnar Tibert, for sharing his knowledge and putting up with all my questions.

Colleagues, especially on the eighth floor, thanks for creating a pleasant environment.

Izabelle Lantz, Anette Nordström, Maria Lysell, Eva and Magnus Torsson, for listening to my problems, without having a clue of what they are.

Pia and Pontus Nilsson, my brother with spouse, and Emma and Eric Schenker, my sister with spouse, always showing great support.

My mom and dad, Christina and Hans Nilsson, for all love, support and help in any situation.

My daughter, Felicia, bringing new light and joy into my life.

Anders my husband and best friend. Thank you for your endless love, support and believe in me!

Dissertation

This thesis is based on the work of two publications. The publications are preceded by an extended introduction to the biomechanics of human movement and the method of evaluation for optimal forces in the musculoskeletal system. A review of the publications is also included. This part is ended by a chapter of conclusions and future work to the studies.

Paper 1. Sofia Heintz, Elena Gutierrez-Farewik and Anders Eriksson. Evaluation of load-sharing and load capacity in force-limited muscle systems. Submitted to *Computer Methods in Biomechanics and Biomedical Engineering*

Paper 2. Sofia Heintz, Elena Gutierrez-Farewik. Evaluation of muscle forces during gait; static optimization and EMG-to-force in comparison. Submitted to *Gait and Posture*

Division between authors

Numerical modelling and experimental setup were done by the respondent with supervision from Prof. Anders Eriksson and Dr. Elena Gutierrez-Farewik.

The optimization algorithm used in both papers was developed by Prof. Anders Eriksson.

Dr. Elena Gutierrez-Farewik, who is also at the Karolinska Institute, Department of Woman and Child Health, provided the use of the Motion analysis lab at Karolinska Astrid Lindgrans Hospital, where the gait analysis was done together with the respondent.

Article texts was written by all three authors.

Contents

Chapter 1

Introduction

1.1 Human Movement

Biomechanics of the human movement can be defined as the inter-discipline which describes, analyzes and assesses human movement [63]. The interest in identification and analysis of the human movement traces back to Aristotle who studied the motion and gait of humans and animals [46].

Common aims of a biomechanical analysis of human motion and the muscles coordinating the motion are to determine the timing of muscle contractions, the amount of force generated and moment of force about a joint, and the type of contraction, concentric or eccentric. Motion data based on video camera tracking system, combined with a mathematical model to describe anatomical movement based on passive marker coordinates, can produce kinematics of movement. If force plates, which measure ground reaction force, are used simultaneously to the camera tracking system, movement kinetics can be evaluated. However, to further understand the human movement the causal relationship between kinematics and kinetics from motion analysis to measured muscle activation must be determined [67].

1.2 Evaluation of Muscle Forces and Function

For a better understanding and identification of the function and structure of the musculoskeletal system, mathematical musculoskeletal computer programs to simulate a movement can be used. The body can be modelled as a multi-body system which is connected by joints and spanned by muscle-tendon actuators. For each joint, there is a redundant set of muscles implying a statically underdetermined system of equilibrium equations, i.e., there are an infinite number of solutions. Solving the system is an complex optimization problem. Both static and dynamic solution methods has been used for this problem over the years [2, 17, 47, 54, 64].

In this study the method used is based on traditional static optimization technique. A numerical algorithm is presented which unifies established optimization techniques in a common algorithm. The algorithm is built in a modular way in Matlab (The Mathworks, Inc., Natick, MA, USA), and is easy adaptable to work together with motion analysis data.

1.3 Scope and Aims

The primary focus in the two presented papers is on the modelling of skeletal muscles with the use of a numerical optimization algorithm. In Paper 1 the focus is on the development of a numerical constrained optimization algorithm to be used in an example evaluating the forces in the upper limb including the elbow and shoulder. Paper 2 aims at applying the developed optimization algorithm to gait, where kinematics and kinetics from experimental gait analysis are used. Validation of evaluated forces is proposed with a method based on electromyography (EMG) activity and normalization.

Chapter 2

Human Movement

2.1 Terminology describing the musculoskeletal system

To describe the human body and its movements anatomical terminology is used. A three dimensional coordinate system consisting of three anatomical planes, sagittal, frontal (coronal) and transverse planes, is used to identify an anatomical position and the axes of motion (Figure 2.1). To describe relative location or directions, spatial and directional terminology is used: *anterior*, toward the front and *posterior*, toward the rear, *superior* indicates toward or closer to the head and *inferior* closer to the feet, *medial* refers to a location closer to the midline of the body and *lateral* refers to a location away from the midline. In describing the extremities, upper and lower, of the body, *proximal* to a positions along a limb with a location closer to the attachment to the body and *distal* refers to a more distant part of the limb away from the body [10, 46].

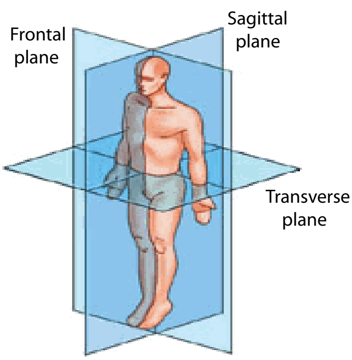

Figure 2.1: The anatomical planes defining the three planes, sagittal-, coronal- and transverse plane.

2.1.1 Kinematics

Kinematic variables describe the movement, independent of the forces that cause the movement. They include linear displacements, d, speed, s, and velocities, v, and accelerations, a, and also angular displacement, Θ, velocities, ω, and accelerations, α [63].

Movement or motion indicates a joint action, the relative angular movement of the limbs on the distal and proximal sides of the joint [46]. By identifying the plane of motion in which direction the action takes place, motions are defined by *flexion* and *extension* occurring when movement around the transversal axes, movement around anteroposterior axes is identified by *abduction* (moving out from the body) and *adduction* (toward the body), movement around the longitudinal axes is called *rotation*, internal and external.

To describe the kinematics of a segment a coordinate reference system is used. Each segment can be set with an origin and a principal axis, which is usually defined along the long axis of the segment. Three dimensional imaging systems are used to detect kinematic data from a subject in a motion analysis. Three types of coordinate systems are used to derive the kinematics, the global reference system (GRS) which remains fixed in space, a technical reference system which is derived from the subject's reflective markers, and an anatomical reference system (ARS) which is attached to each body segment [29].

A moving segment's translation and rotation, are described by the segment's ARS position and orientation relative to the GRS. In two dimensional translation of a point, a, in the ARS, (x_i, y_i), relative to the GRS, (X_i, Y_i), can be written as [63]:

$$\begin{bmatrix} X \\ Y \end{bmatrix}_a = \begin{bmatrix} X \\ Y \end{bmatrix}_i + \begin{bmatrix} c & -s \\ s & c \end{bmatrix} \begin{bmatrix} x \\ y \end{bmatrix}_{ia} \tag{2.1}$$

Where s is denoting sine and c cosine of an angle (θ).

A rigid body moving in a three dimensional system, has a possibility of translations and rotations. This implies a 3×3 transformation matrix, $[\phi]$. A common angular system used to define the angular orientation in space is the Euler system of angles. A specific definition of Euler angles will describe in which sequence the rotations take place [63]. Euler's convention contain 12 different sequence of rotations [68].

An axis system denoted by x, y, z will be transformed into a system denoted by $x^{'''}, y^{'''}, z^{'''}$ in a chosen sequence. The Cardan system, $x-y-z$, which is common in biomechanics, describes the sequence order of axes to rotate about (Equations 2.2 and 2.3) [63]. The first rotation, θ_1, is about the x axis to get x', y', z'; the second rotation, θ_2, is about the new y' to get x'', y'', z''; and the last rotation, θ_3, is about z'' to get to x''', y''', z'''.

An assumed point in the original x, y, z axis system with coordinates x_0, y_0, z_0, will have coordinates x_1, x_1, x_1 in the x', y', z' axis system, based on rotation θ_1. The second rotation θ_2 will provide coordinates x_2, y_2, z_2 in the axis system x'', y'', z'', and the final rotation θ_3 will provide the point the coordinates x_3, y_3, z_3 in the axis system x''', y''', z'''. These rotation can be written:

$$[\phi_1] = \begin{bmatrix} 1 & 0 & 0 \\ 0 & c_1 & s_1 \\ 0 & -s_1 & c_1 \end{bmatrix}, \quad [\phi_2] = \begin{bmatrix} c_1 & 0 & -s_1 \\ 0 & 1 & 0 \\ s_2 & 0 & c_2 \end{bmatrix}, \quad [\phi_3] = \begin{bmatrix} c_3 & s_3 & 0 \\ -s_3 & c_3 & 0 \\ 0 & 0 & 1 \end{bmatrix} \tag{2.2}$$

where (c_1, s_1), (c_2, s_2) and (c_3, s_3) denote (sinθ_1, cosθ_1), (sinθ_2, cosθ_2), and (sinθ_3, cosθ_3) respectively.

The transformation of the point from the axis system x, y, z to x''', y''', z''' can then be written [63]:

$$\begin{bmatrix} x_3 \\ y_3 \\ z_3 \end{bmatrix} = [\phi_3][\phi_2][\phi_1] \begin{bmatrix} x_0 \\ y_0 \\ z_0 \end{bmatrix} \tag{2.3}$$

2.1.2 Kinetics

Kinetics deals with the forces associated with a movement. Internal forces come from muscle activity, tendons and ligaments, and joint contact forces and external forces comes from ground reaction forces, segment weight, or applied loading on the musculoskeletal system [63]. Knowledge of the muscle forces is important for understanding the causes of movement. Kinetic quantities are evaluated from kinematics, anthropometric data and external forces, such as the ground reaction force, f_{GRF}, [63].

Newton's second law of motion (Equation 2.4) together with the Euler dynamic equation (Equation 2.5), make up the basis for the mathematical model of the limbs called link-segment modelling using inverse dynamics, where reaction forces, R, and muscle moments, M, are calculated [63, 69]:

$$R = m \cdot a \tag{2.4}$$

$$M = I \cdot \alpha \tag{2.5}$$

where m is the mass of the object, a is the linear acceleration, I, is the mass moment of inertia and α is the angular acceleration of the object.

The link-segment model is broken down at the joints into segments which are treated separately as rigid bodies, creating a free-body diagram (Figure 2.2) [41]. In accordance to Newton's third law, there is an equal and opposite force acting at each joint, and moment and forces can be evaluated at any joint with a known external loading or reaction force. Modelling the limb in this way carries the assumptions that (1) each segment has a fixed mass located at its center of mass (in the center of gravity) (2) the location of each segment's center of mass (COM) remains fixed (3) joints

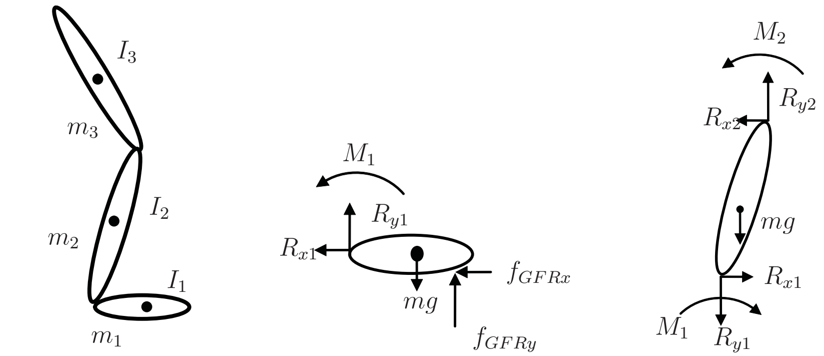

(a) Link segment (b) Foot segment (c) Shank segment

Figure 2.2: Link-segment modelling and free body diagram of the foot- and shank segment, showing moments of inertia, I_i, masses, m_i, reaction forces, R_{yi} and R_{xi}, joint moments, M_i, $i = 1, 2, 3$. Calculation of moment and forces via inverse dynamics (Equations 2.6 and 2.7)

are considered without translations (4) mass moment of inertia of each segment is constant and (5) the length of each segment is constant during movement [63].

The method of inverse dynamics is usually employed in gait analysis to compute the net joint moments, net joint powers and intersegmental forces. Evaluation starts at the foot segment (Figure 2.2(b)) with the ankle joint forces and moment (Equations 2.6 and 2.7) [41]. Establishing the forces in the y direction and the moment about the ankle, M_1:

$$\sum R_{y1} = m_1 \cdot a_{y1} = f_{GRFy1} + R_{y1} - mg \tag{2.6}$$

$$\sum M_1 = I \cdot \alpha = f_{GFRy} d_{GRF} + R_{y1} d_{y1} + M_1 \tag{2.7}$$

where d_{GRF} describe the moment arm of the ground reaction force f_{GRFy} to the ankle joint and d_y the moment arm to the reaction force R_{y1} to the ankle joint. The carry weight mg is located at the center of mass (CoM), moment of inertia, I, is evaluated from anthropometric tables and linear and angular acceleration, a and α, are obtained from kinematic data. From this point the knee joint moment and forces can be evaluated by applying equal and opposite reaction force on the shank segment (Figure 2.2(c)) [41].

2.2 Muscle Architecture

According to Lieber and Friden [44], muscle architecture is the primary determinant of muscle function. Understanding this structural and functional relationship is of great practical importance to provide a basic understanding of the physiological

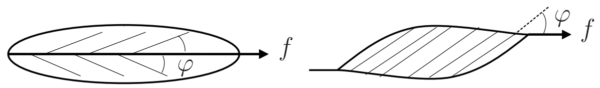

(a) Pennate muscle (b) Multipennate muscle

Figure 2.3: Schematic figures on two way of muscle fiber arrangement showing the angle of pennation, α, in relation to the axis of force, f. Skeletal muscle function is defined as "the arrangement of muscle fibers within a muscle relative to the axis of force generation" [43].

basis of muscle force production in human movement. Skeletal muscle architecture is defined as "the arrangement of muscle fibers within a muscle relative to the axis of force generation" (Figure 2.3) [43].

The muscle's architectural properties are often measured in experimental microdissection of whole muscle [44]. Pennation angle, φ, is determined by the angle of the muscle fibers relative to the muscle's axis of force generation. Pennation angle in human upper and lower limb skeletal muscles usually varies from 0 degrees to 32 degrees and muscle fiber length variation varies approximately from 20 to 500 mm [25, 26]. According to Lieber [43], muscle length is defined as the distance from the origin of the most proximal muscle fibers to the insertion of the most distal fibers. Fiber length ,l_f, is usually estimated from bundles consisting of 10 to 100 fibers, because of the difficult process in isolating a single fiber [44]. With the described muscular properties, together with the volume of the muscle, V_m, the physiological cross-sectional area (PCSA) can be evaluated:

$$PCSA = V_m cos(\varphi)/l_f \tag{2.8}$$

In the evaluation of muscle volume a density of $1.0597 \cdot 10^3$ kg/m^3 is usually used [43, 62].

PCSA is proportional to the maximum tension generated by the muscle and is the major determinant of a muscle's strength [52, 56]. The functional difference of two muscles with identical fiber length and pennation angles but with different PCSA (large and small) is illustrated in (Figure 2.4).

PCSA values reported in the literature tend to vary considerably for some muscles. Recent studies have shown that due to dehydration effects on cadaver specimens, reported PCSA data can have a 5–10 percent error [60]. An additional factor to consider is measurement of muscle volume, which has been reported to lead to significant errors in the evaluated PCSA [27]. Using magnetic resonance imaging (MRI) techniques PCSA can be evaluated with in-vivo measures of muscle volume, but that will exclude measures of pennation angle from the examined muscle [28]. The reported PCSA values measured from MRI studies are greater than those from cadaver studies [26].

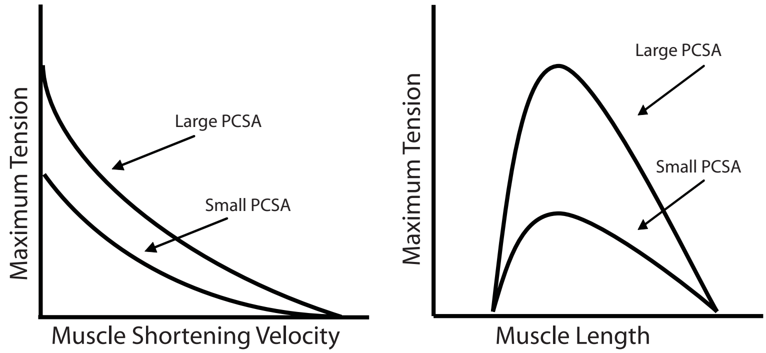

(a) Tension–Shortening Velocity (b) Tension–Length

Figure 2.4: The architectural properties of two muscles with small respective large PCSA (a) showing the tension–shortening velocity relationship of a muscle in concentric contraction (b) showing the tension–length relationship of the active muscle in concentric contraction [44].

2.2.1 Musculoskeletal system functions

A movement is usually a collaboration of a set of muscles, where every individual muscle exerts a specific amount of force and in a specific direction. The *agonist* is the prime mover of exerted movement. Together with the agonist, *synergistic* muscles work to support the movement in a concentric, or shortening, contraction. The *antagonists* exert eccentric, or lengthening, contraction, providing stability to the movement. This phenomenon is sometimes called *co-contraction*, and is defined as the presence of antagonistic muscle activity.

Characteristic properties of the upper and lower extremity muscles are often grouped to their functions, for example hip flexors and extensors, knee flexors and extensors, dorsiflexors and plantarflexors in the lower limb. In the extremities a functional group is usually supported by its own nerve [10].

A muscle can only produce tension. The muscles are usually united in functional chains where muscles can work as an extension of each other, such as the trapezius and deltoideus, or as antagonist couples, such as soleus and tibialis anterior which work together to create stability of the ankle joint and positioning of the foot. Biarticular muscles are crossing two joints, exerting influence on the movement in both.

2.2.2 Musculoskeletal Modelling

Force produced by a muscle can be simulated in different ways. The most common numerical description of a muscle model is called the Hill-model after its founder A.V. Hill in 1938 [49,63]. This mathematical relationship represents muscular shortening (concentric contraction):

$$(F + a)(V + b) = (F_0 + a)b \tag{2.9}$$

where, F represents force, V represents velocity, a is coefficient of shortening heat, b stands for $a \cdot V_0/P_0$, where V_0 is maximum velocity and F_0 is maximum isometric tension. This relationship represents the characteristics of a muscle in concentric contraction, the tension decreases with increasing shortening velocity under load. The curve describing this effect is called a force–velocity curve (Figure 2.4(a)). In the expression, the muscle is assumed to be fully activated.

In describing the mechanical components of a muscle in motion, a three component Hill model is often used [66]. This model represents a muscle contraction in a mechanical formulation, which is reasonably correct for several simulation contexts.

The model includes several known mechanical properties, such as the force–length relationship of fiber and tendon length and the force–velocity relationship, which will make the muscle force evaluation of the simulation realistic. The three component Hill model consists of a contractile element (CE), representing the muscle fiber, and two non-linear elastic elements, a parallel elastic element (PEE), representing passive properties of surrounding tissue, and a series elastic element (SEE), representing the tendon and other elastic tissues [49].

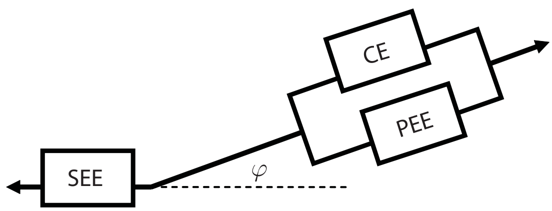

Figure 2.5: The generic Three component Hill-type muscle-tendon model described by Zajac in (1989) [65]. The model consist of one active contractile element (CE) in parallel with a passive elastic element (PEE), and in series with one non-linear elastic element (SEE) which is modelled with a pennation angle α.

A muscle-tendon actuator model based on the tree component Hill-model was proposed by Zajac in 1989, including a pennation angle α (Figures 2.5 and 2.6) [65]. Muscle architectural properties of the muscle force–fiber length, the muscle force–fiber velocity and tendon force–tendon length relationships, together with peak isometric force, optimal muscle fiber length and pennation angle at optimal fiber length, tendon slack length and maximum shortening velocity are used as inputs to the model. Muscle architectural properties were obtained from experimental studies.

Zajac's model is used in a computer program (SIMM, Musculographics Inc., Santa Rosa, CA, USA) to visualize whole body models [20, 21]. This is a generic model which scales a specific musculotendon actuator, so that its force-length relationship can be evaluated. The model also take pennation angle into account. Musculotendon

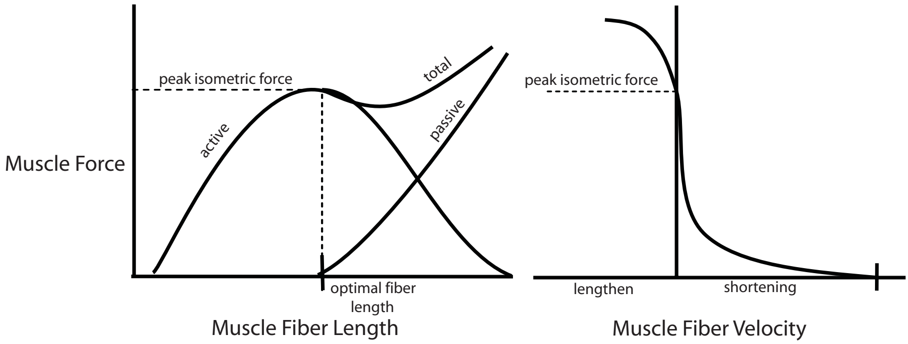

Figure 2.6: Schematic figure of the muscle properties used by the Three component Hill-type muscle-tendon actuator model described by Zajac in (1989) [65].

paths are modelled as a series of line segment, with large attachment areas divided in compartments. However, recent studies on moment arms and muscle attachment modelling in a three-dimensional representation show great potential more accurate modelling of the muscle paths [7].

2.3 Motion Analysis

The method of visualizing motion began in the early 1800s when the Weber brothers investigated muscle contractions and their role in human walking [12]. A biomechanical analysis of the human motion is usually based on visual observation, recorded kinematics and kinetics data and electromyography (EMG) analysis [63].

2.3.1 Gait Analysis

Walking is arguably the most convenient way to travel short distances. Normal walking is extremely energy efficient. The typical energy produced in normal gait is 10.5 kJ per minute. Deviation from the normal gait pattern will increase this energy cost. For example, fast walking will give an 60 percent increase [30].

A gait cycle is defined as the movement of a single limb from foot-strike to foot-strike again [29]. It is often seen as eight phases, initial contact, loading response, mid stance, terminal stance, pre-swing, initial swing, mid swing, terminal swing [51].

Gait analysis is the evaluation of a human walking pattern. In the analysis the walking patterns are documented by different measurement techniques. Cameras linked to a computer system are used to record the kinematics. Markers on a subject reflect light, which is digitized and processed on the computer. Ground reaction force is measured from force plates, then joint moments are evaluated via

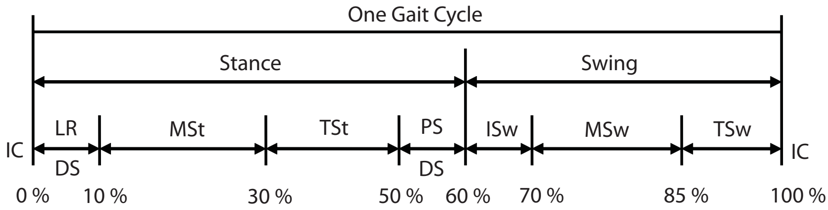

Figure 2.7: One Gait Cycle. First divided in two periods, stance and swing. Second, the gait cycle is divided in eight phases, initial contact (IC), loading response (LR), mid stance (MSt), terminal stance (TSt), pre swing (PS), initial swing (ISw), mid swing (MSw), terminal swing(TSw). The two periods of double limb stance (DS) are pointed out [51].

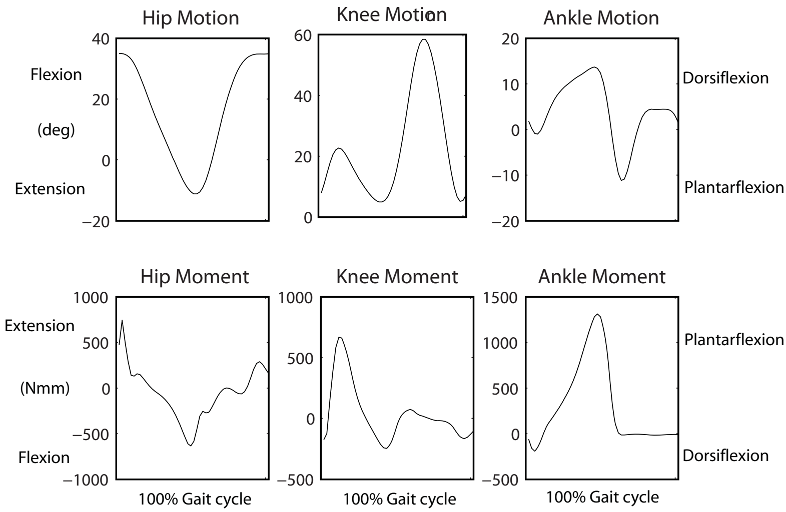

Figure 2.8: Normal gait data, the first row shows lower limb sagittal angular motion at the hip, knee and ankle joint. The second row shows sagittal moment in the respective joint. All data represent one gait cycle. (Obtained from the Motoriklab at Karolinska University Hospital)

inverse dynamics. The results from gait analysis are typically joint angles and joint moments (Figure 2.8).

The requirements of normal gait according to Gage [29] are: (1) stability of the foot and the ankle, (2) clearance of the ground by the foot in swing phase, (3) proper pre-positioning of the foot in terminal swing, (4) adequate step length and (5) maximization of energy conservation.

The advantages to gait analysis are that gait is well defined and predictable making it easy to identify deviation. The information from gait analysis, kinematic and kinetic

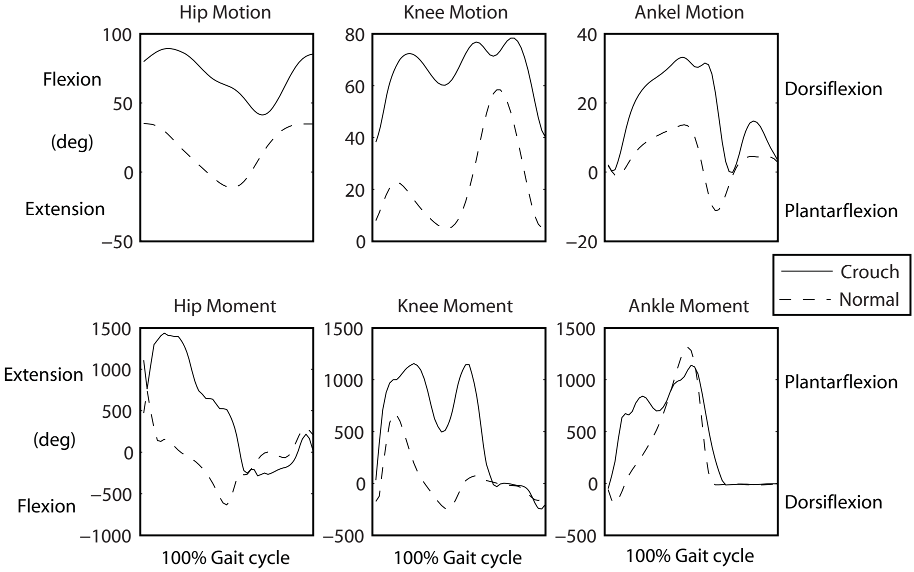

Figure 2.9: Crouch gait data, from a healthy subject imitating crouch gait. The first row shows sagittal angular motion at the hip, knee and ankle joint. The second row shows sagittal moments in the respective joint. All data represents one gait cycle. (Obtained from the Motoriklab at Karolinska University Hospital)

and also EMG, together with physical examination data help to clarify the cause of deviation from normal gait [33]. This enables better decisions on the best way to treat patients with different pathological disorder [51]. The most represented and the most recognized pathological disorder is cerebral palsy, where great knowledge has been gained about the treatment decisions [29]. Figure 2.9 shows the deviation in gait patterns from a healthy subject imitating crouch gait. Crouch gait is a typical gait pattern recognized in subjects with cerebral palsy, which is an excessive flexion in the hip and knee angle usually caused soleus weakness as a result from tendon-Achilles lengthening [29].

2.3.2 Electromyography

The activation of a skeletal muscle during movement can be shown by EMG recordings. The net EMG signal is an algebraic summation of the electrical potentials known as motor unit action potentials (MUAPS) that are generated when a muscle contracts [29]. A motor unit consists of a single controlling neuron and the motor nerve cell in the spinal cord, which innervates an ensemble of muscle fibers [51]. In response to an action potential from the motor unit, a muscle fiber depolarizes as the signal propagates along its surface and the fiber twitches, i.e., the muscle contracts [29, 63]. This depolarization generates an electric field in the vicinity of the muscle fibers which can be detected by an EMG electrode [35].

There are several causative factors which have more or less effect on the EMG signal. Extrinsic causative factors are related to the electrode placement and structure. The number of active motor units detected and possible amount of cross-talk from nearby muscles depend on the location of the electrode [19]. Intrinsic causative factors are dependent of physiological, anatomical and biochemical characteristics of the measured muscle [19]. The major intrinsic factors are; the number of active motor units, i.e., the more a muscle contracts the more active motor unit action potential, which will contribute to the magnitude of the EMG signal, fiber architecture, such as diameter, location of the active fibers, and fiber type composition.

EMG recordings are obtained with surface electrodes or with indwelling electrodes, proximal wire or distal wire. What determines the choice of electrodes is the muscle of interest and the purpose of the EMG recordings. Indwelling electrodes are more selective in detecting MUAPS than surface electrodes, due to the small sensing area and are able to analyze muscle activity in deep or small muscles [8, 35, 51]. They, however, can be inconvenient to use as the insertion process is invasive. Surface electrodes detect MUAPS in a larger area, but the possibility increases to detect activity in muscles other than the desired muscle, cross-talk. It has been shown that EMG data from surface and indwelling during stance phase resulted in remarkably similar EMG profiles [8].

The EMG the raw signal can be processed in order to, e.g., compare the recorded muscle activation with a biological or biomechanical variable.

2.3.3 Signal Processing

The unprocessed recorded EMG signal is called raw data. This data also contain noise from many sources such as electrical disturbance and interference. All noise will result in errors in the EMG data, therefore it is necessary to analyze and smooth the data. Analyzing the EMG signals can be done in the time domain and the frequency domain. The noise of a signal is often a combination of a periodic and a randomly alternating signal, and can also have a component of direct current. Its frequency content or its harmonic components are analyzed by using Fourier series. The mathematical process to perform this is called Fourier transform [42].

Evaluation of the frequency spectra is useful in detecting noise in the signal. This analysis can also be useful in analyzing fatigue [19, 63]. EMG data of fatigue is shown as a decrease in the frequency spectra.

Further processing of the raw EMG signal, to be comparable to a biomechanical variable, is done in the time domain. Filtering of the signal aims at the rejection, or attenuation, of unwanted frequencies. A low-pass filter attenuates high frequency data and high-pass filter, low frequencies.

To interpret the data the signal can be filtered. Numerous ways are described in the literature to process EMG signals when representing muscle activation patterns

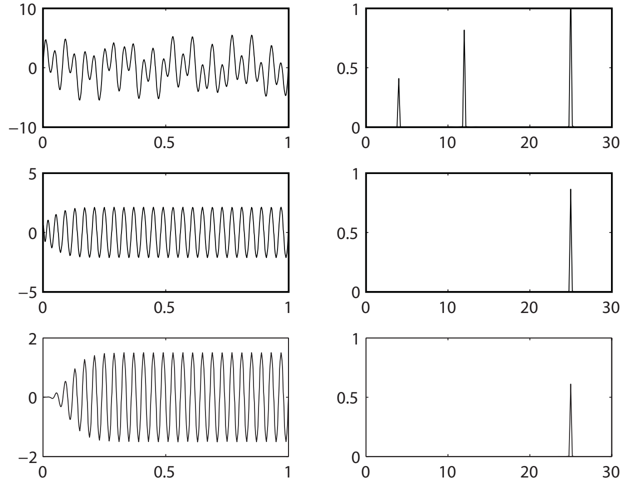

Figure 2.10: Signal processing of a made up sine signal, showing the raw signal and its frequency content in the first row, at second row the signal is high-pass filtered at 25 Hz together with its frequency content on its right, and last row is showing the signal low-pass filtered at 5 Hz together with its frequency content.

[19, 35, 63]. However, in many motion labs the raw signal is used to describe the force patterns as just 'on' or 'off', with an introduced threshold activity as the borderline [9, 29].

A common way to present the EMG signal is as an linear envelope of the signal, i.e., an absolute value of the filtered EMG signal. Common methods are described by Winter [63] and Hof et al. [36], and are also used in Paper 2. In these methods the raw EMG signal is first filtered with a high-pass Butterworth filter, then full wave rectified, and lastly filtered by a low-pass Butterworth.

Figure 2.10 shows an example in the development of the linear envelope. A set of sine waves at different magnitudes, hence, representing a raw signal, are processed and presented in the time domain together with its frequency spectrum. Three steps are shown: the raw data, high-pass filtered data at 25 Hz and low-pass filtered data at 5 Hz.

In applying the method to EMG activation, the linear envelope was calculated over a range of two gait cycles, i.e., from 50% of the prior and up till 50% of the subsequent gait cycle. This is done to avoid the signal to be constrained to zero at the beginning of the cycle, which is a consequence of the filtering process. Figure 2.11 show signal processing of EMG from the soleus muscle.

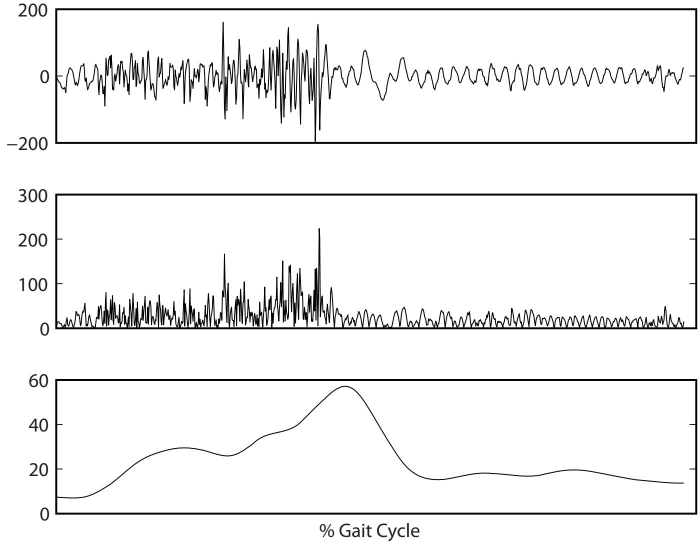

Figure 2.11: Soleus EMG signal, showing the signal processing in three steps: (1) the raw signal, (2) high-pass filtered at 25 Hz and full-wave rectified, (3) low-pass filtered at 5 Hz.

2.3.4 EMG Normalization

Numerous authors describe methods to normalize an EMG signal [9,37]. In our study on lower limb muscular forces the gait EMG signal was normalized by maximum voluntary contraction (MVC), as previously described by Bogey et al. [9].

MVC tests were executed in a strength measuring chair (SMC) [23]. The SMC measures the strength in the lower limbs in plantarflexion, dorsiflexion, knee flexion and knee extension. Strength can be estimated via force sensors which measure the compression or tension under the foot and at the ankle (Figure 2.12).

Simultaneous EMG was recoded to estimate the EMG activity level at the MVC. The body was seated in an upright position with the hip and ankle angles in 90 degrees flexion and the knee in a variable angle between 60 degrees and 90 degrees flexion. Straps were used to restrain the movement at hip, thigh, ankle and foot. Plantarflexor muscle strength is estimated by exerting compression on the force sensor under the foot. Dorsiflexor muscle strength was tested by lifting the foot. Knee flexor and extensor muscles was tested in a restrained flexion and extension while exerting tension or compression on the force sensor behind the calf.

Signal processing of the recorded EMG during the MVC trials was done in the same way as the processing of the EMG data from gait analysis. After the linear envelope, a one second sliding mean was evaluated and the maximum mean from a number of trials were used to normalize the gait EMG.

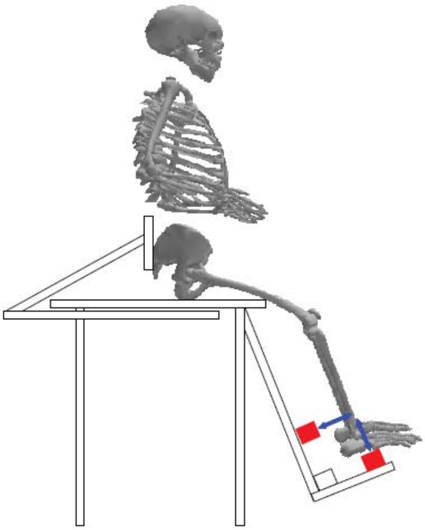

Figure 2.12: Drawing of the strength measuring chair (SMC), from Farewik [23] with permission. Straps will lock the subjects position at the hip, knee, foot and ankle. Force sensors are located at the ankle and under the foot, and are visualized as squared boxes.

Chapter 3

Muscular Force Distribution

3.1 Optimization of Muscular Forces

3.1.1 Background

Individual muscular forces are difficult to measure accurately and there is no practical way to estimate muscular forces for a whole or even a part of a system, such as the upper or lower limb. Mathematic modelling can be used to predict these desired individual muscular forces.

The musculoskeletal system is mathematically a redundant force system. This implies an underdetermined system, a system which has more unknown forces than equilibrium equations. This will exclude the possibility of a unique solution for muscle forces and joint reactions in each position [16]. Optimization theory is believed to give good indications of the physiological basis underlying muscular force-sharing function in many musculoskeletal structures [49].

The optimization of the muscular forces in a static or dynamic configuration can be based on different standard mathematical methods, and on different criteria for optimal behavior. It has been shown that even though the human body and its muscles are dynamic motors of the musculoskeletal system, static optimization is often relevant and gives satisfactory results, depending on desired evaluation and purpose of study [2]. Dynamic forces are then seen as static in every time instant.

Over the years numerous studies of optimization theory have been performed with the purposes to evaluate muscular forces with a mathematical optimization method [1, 3, 16, 17, 22, 40, 50, 54, 55, 57, 64].

When modelling the musculoskeletal human body, a set of force or moment equilibrium equations, $\mathbf{Ax} = \mathbf{b}$, is formulated at the joints of the modelled structure, with $\mathbf{x}$ representing the unknown muscular forces. This set of equilibrium equations, together with limiting values of the muscular maximum tension constrains the system. Unloaded states are assumed to have zero forces in all muscles, $\mathbf{x} = 0$, which is not necessarily true, since in many common situations antagonistic muscles are active but the resulting net force or moment is zero [24].

3.1.2 Optimization Theory

An underdetermined system can be solved with optimization theory. The optimal solution of a system is an admissible solution $\mathbf{x}$ of minimum cost where a suitable cost function, $\mathcal{C}(\mathbf{x})$, can be chosen rather freely [58].

For a system constrained by equality equations, such as equilibrium equations, redundant force systems can, under some assumptions, be solved by using the Moore-Penrose pseudo-inverse $\mathbf{A}^+$ to a matrix $\mathbf{A}$ [59], Yamaguchi et al. applied this method to the evaluation of muscular forces [64]. This classical numerical method solves an underdetermined system $\mathbf{Ax} = \mathbf{b}$, to yield the solution $\mathbf{x}$ with minimum Euclidean norm [59]:

$$\parallel \mathbf{x} \parallel = ({x_1}^2 + {x_2}^2 + ... + {x_i}^2)^{1/2} \tag{3.1}$$

This will only work for a certain type of cost functions, where:

$$\mathcal{C}(\mathbf{x}) = \sum_i (x_i)^2 \tag{3.2}$$

As the muscles can only generate positive forces, constraints will be necessary on the system. This optimization problem is typically formulated as:

$$\text{minimize } \mathcal{C}(\mathbf{x}) \tag{3.3}$$

$$\text{subject to } \mathbf{h}(\mathbf{x}) = \mathbf{0} \qquad \text{and} \qquad \mathbf{g}(\mathbf{x}) \leq \mathbf{0} \tag{3.4}$$

where $\mathcal{C}(\mathbf{x})$ is the cost function of the unknowns, $\mathbf{h}(\mathbf{x})$ states a set of equality constraints and $\mathbf{g}(\mathbf{x})$ a set of inequality constraints, [6]. In the present context, equilibrium equations give the equalities, whereas the ranges of possible muscular forces give the inequalities.

A system based on equilibrium equations, $\mathbf{Ax} = \mathbf{b}$, together with a cost function, $\mathcal{C}(\mathbf{x})$, can be solved with the help of Lagrange multipliers. They convert the constrained minimization of $\mathcal{C}(\mathbf{x})$ into an unconstrained minimization [48, 58]. This leads to:

$$\mathcal{L}(\mathbf{x}, \boldsymbol{\mu}) = \mathcal{C}(\mathbf{x}) + \boldsymbol{\mu}^T(\mathbf{Ax} - \mathbf{b}) \tag{3.5}$$

where $\mathbf{Ax} - \mathbf{b}$ represent the residual of the equilibrium equation, and $\boldsymbol{\mu}$ is a set of Lagrange multipliers.

Consider a two-link segment with three muscles spanning one joint (Figure 3.1). The moment equilibrium equation of the system will then constrain the system. The chosen cost function is the sum of the forces squared. The forces f_1, f_2, f_3 are

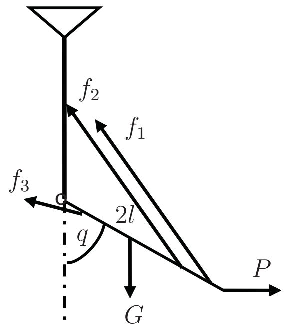

Figure 3.1: Free-body diagram of an example of a simple model of the elbow joint in a fixed geometry,

then the unknown in $\mathbf{x}$, and must be chosen to carry the forces P and G. Only one equilibrium equation can be formulated for the unknowns, so the system is redundant and unknowns can be optimally chosen.

The moment equilibrium constraint is written as one part reflecting the load carried by the system, $\mathbf{b}$, and one part with the unknown muscular forces, $\mathbf{Ax}$, with their respective moment arms:

$$\mathbf{b} = Gl \sin q - 2Pl \cos q \tag{3.6}$$

$$\mathbf{Ax} = f_1 d_1 + f_2 d_2 - f_3 d_3 \tag{3.7}$$

where:

$$\mathbf{x} = \begin{pmatrix} f_1 & f_2 & f_3 \end{pmatrix} \tag{3.8}$$

and d_1, d_2, d_3 are the moment arms of the muscular forces, f_1, f_2, f_3, with their relevant signs. The cost function for the two-link segment model of the elbow can then be written:

$$\mathcal{C} = ({f_1}^2 + {f_2}^2 + {f_3}^2)/2 \tag{3.9}$$

The Lagrange equation, (Equation 3.5), can then formed and the minimum is sought. The constrained minimal solution is then predicted by setting the differentials of the Lagrange equation to zero:

$$\begin{pmatrix} \mathcal{L}_{,\mathbf{x}} \\ \mathcal{L}_{,\boldsymbol{\mu}} \end{pmatrix} = \mathbf{0} \tag{3.10}$$

With additional constraints, such as minimum or maximum values for the unknown, an extra set of Lagrange multipliers can be added to the Lagrange equation:

$$\mathcal{L}(\mathbf{x}, \boldsymbol{\mu}) = \mathcal{C}(\mathbf{x}) + \boldsymbol{\mu}^T(\mathbf{Ax} - \mathbf{b}) + {\boldsymbol{\mu}_L}^T \mathbf{x}_L \tag{3.11}$$

In the example, if f_i are not allowed to become negative, the constraints $f_i \geq 0$ is introduced by including in $\mathbf{x}_L$ the components f_i.

3.1.3 Performance Criteria

Various optimization approaches have been used to solve the redundant muscular force system. The main differences are how the cost function is set up, and in the choice of solution method. In a biomechanical context, the cost functions are sometimes called performance criteria, to represent the performance which minimizes the activation of the muscular system. The assumption is that the body selects muscles for a given activity according to the performance criteria chosen.

The typical performance function is the sum of muscular stresses or forces raised to a power:

$$\mathcal{C}(\mathbf{x}) = \sum_i c_i {x_i}^n \tag{3.12}$$

where x_i is the muscular stresses, σ_i, or forces, f_i, of the system, n is an arbitrary integer > 1, and c_i can be used as weighting factors.

Table (3.1) gives an overview of optimization studies on different musculoskeletal systems together with the chosen performance criteria and the solution methods

Table 3.1: Overview of some used performance criteria for minimization with the connected solution method in biomechanical optimization studies.

System	Criteria $\mathcal{C}(\mathbf{x})$	Solution method	Ref.	Note
Lower Limb	$\sum_i {x_i}^n$	Simplex method and Lagrange method	[22]	^{a}
	$\sum_i {x_i}^n$	Nonlinear programming	[16]	^{b}
	$\sum_i \alpha_i$	Linear programming	[40]	^{c}
Gait	$\sum_i f_i + 4\sum M_i$	Simplex method	[57]	^{d}
	$\sum_i (f_i/f_{\max i})^2$	Linear programming approach	[50]	
	$\sum_i {\sigma_i}^3$	Rosen's gradient projection algorithm	[17]	
	$\sum_i c_i {\sigma_i}^2$	Gradient sequential quadratic programming	[3]	
Upper Limb	$\sum_i \alpha_i$	Linear programming	[1]	^{e}
	$\sum_i {\sigma_i}^2$	Pseudo-inverse algorithm	[64]	
	$\sum_i V(f_i/f_{\max} i)^2$	Inverse dynamic optimization	[34]	^{f}
	$\sum_i (fj_i + fl_i)$	Simplex method	[15]	^{g}
	$\sum_i c_i {f_i}^n, n > 1$	Lagrange multiplier method	[54]	
	$\max(f_i/N)$	Simplex method	[55]	^{h}
	$\sum_i {x_i}^n$	Lagrange method, nonlinear programming	[Paper1]	^{i}

^{a}x can be forces or stresses, $n = 1$, 2 or 3
^{b}x can be forces or stresses or instantaneous power, ΔW, n is an arbitrary integer > 1
^{c}α is the activation, describing the number of active motor units, varies between 0 and 1
^{d}M is the moment at all the joints included in the system
^{e}α is the upper bound value of the overall activation of all muscles
^{f}V is the volume of each muscle
^{g}where fj are joint contact forces and fl are the ligament forces
^{h}N are normalization factors or functions
^{i}x can be forces or stresses, $n = 1$, is an arbitrary integer > 1

connected with them. Paper 1 investigates some different performance criteria and their influence on evaluated force values.

A recent study by Praagman et al. (2006) proposed a new and different variation of cost function based on an energy relationship:

$$\mathbf{C}(\mathbf{x}) = \sum_i E_{mi} \tag{3.13}$$

In the equation E_{mi} represents the muscle energy consumption, and is based on the detachment of cross bridges and re-uptake of calcium, which can be written as a function of muscular forces. The model showed good results in comparison with the classic minimization of muscular stresses [53].

3.1.4 Solution Method

A solution method is typically connected to the optimization of a system of equations. Linear programming solves a linear system with a condition that locks $\mathbf{x}$ at nonnegative solutions of the equilibrium equation [58]. The simplex method is the most common sequence of solving linear programming problems.

When the system to minimize becomes nonlinear, the simplex method will only work in limited cases, when the performance criterion is quadratic. A general nonlinear programming algorithm can be defined and a Newton-type iteration method can be used (Paper1). There also exist a large number of general optimization algorithms, which more or less easily can be adapted for the considered problem class.

3.2 Validation Possibilities

There is no direct way to validate the individual muscular forces producing a movement. The EMG recordings measure the activation of the muscle and are not to be confused with muscular force.

3.2.1 EMG-to-force

A linear relationship between the muscle isometric force and the mean rectified value of the EMG signal can be assumed in a method to evaluate muscle force from isometric contractions [35, 61]. Bogey et al., [9], describe the evaluation of the forces during active muscle contraction as the muscle's maximum muscle force (contractive plus passive elastic components) scaled by the muscle activation from EMG data, called the EMG-to-force processing approach. The method uses EMG data which is linearly enveloped and normalized with their measured maximum voluntary contraction, the muscular forces are then estimated by multiplying maximum isometric forces and normalized EMG data. Maximum muscle forces are collected from the musculoskeletal modelling software (SIMM), which uses a Hill model developed by Zajac [65].

3.2.2 Intramuscular pressure sensors

In an attempt to quantify the relationship between intramuscular pressure (IMP) and force during isometric muscle contraction, length-tension experiments have been reported on the tibialis anterior of a rabbit using fiber optic pressure transducers [18]. Established pressure-time curve suggests that IMP accurately predicts muscle forces under the condition of the study. The transducer used was 0.10 mm^2 and represented about 0.2% of the muscle area, and provides a valuable research tool.

Validation with intramuscular force transducers is promising, but is unfortunately not yet an appropriate method for a clinical test routine, as it requires invasive procedures.

Chapter 4

Review of Papers

This licenciate thesis is based on two papers, both with the purpose to evaluate individual muscular forces in static positions, and during movement. This chapter provides a review of each paper and an extended description on the models used, the upper (Paper 1) and lower limbs (Paper 2).

4.1 Paper 1

The static optimization algorithm developed for accurate force decomposition was used in a numerical example to study the force distribution in variable static configurations of the arm.

The redundancy of the human musculoskeletal system implies that the load-sharing in a muscle function group changes depending on loading capacity of the individual muscles and on the configuration, meaning a possible redistribution of load-carrying when one muscle reaches its maximum capacity. The use of static optimization in modelling the arm to examine the load-sharing properties of the individual muscles is relatively easy to use and is easily adaptable to a wide range of problems.

4.1.1 Model description

The upper limb is modelled as a two segment-link model with 20 muscles and two joints including the shoulder and the elbow (Figures 4.1 and 4.2). Positions were studied in the sagittal plane, as illustrated in two examples. One example is based on a model involving 20 muscles and examines the total loading capacity of the system, and one model contains eight muscles and illustrates in details how the system can be used to understand load-sharing and how synergistic muscles can redistribute load.

Musculoskeletal properties were obtained from a upper limb model developed by Holzbaur et al. [38] for use in the commercially available software (SIMM, Muscu-lographics Inc, Santa Rosa, CA) [20, 21].

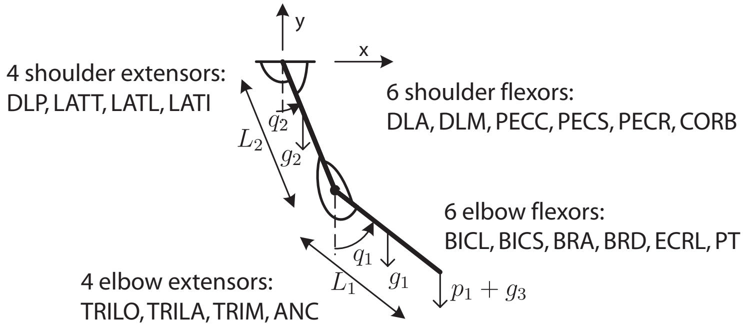

Figure 4.1: Upper limb, free-body diagram

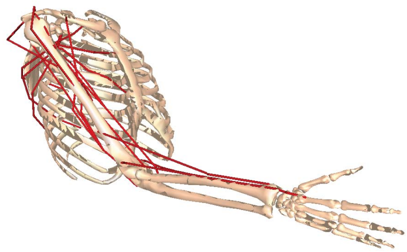

Figure 4.2: Upper limb, image from SIMM [20], model developed by Holzbaur et al. [38]

The range of configurations considered for the numerical experiment were described in segment angles. Range of motion in elbow angle was 0° to 130° and the shoulder angle was -35° to 180°, where a positive angle is anterior to a vertically hanging upper arm. Moment arms of the skeletal muscles vary with joint angle [43, 45]. When modelling the moment arms in the musculoskeletal system, the muscle path is usually modelled with wrapping points, i.e., points in the reference system where the muscle wraps over bone or is constrained by retinacula [20]. Wrapping surfaces are also used to characterize anatomical constraints at the joints [38]. For the studied case, this method in SIMM made the moment arms at the two joints of all considered muscles become mutually independent (Figures 4.3 and 4.4).

Muscle's peak force is evaluated by multiplying the muscle PCSA (Table 4.1) with an assumed maximum specific tension. Specific tension is a measurement of force per unit of muscle cross sectional area. In the upper extremity model developed by Holzbaur et al. a specific tension of 1400 kPa is used in the shoulder and elbow. This relatively high value of specific tension is argued by the author whereas a consequence of disuse atrophy associated with the elderly population, from which

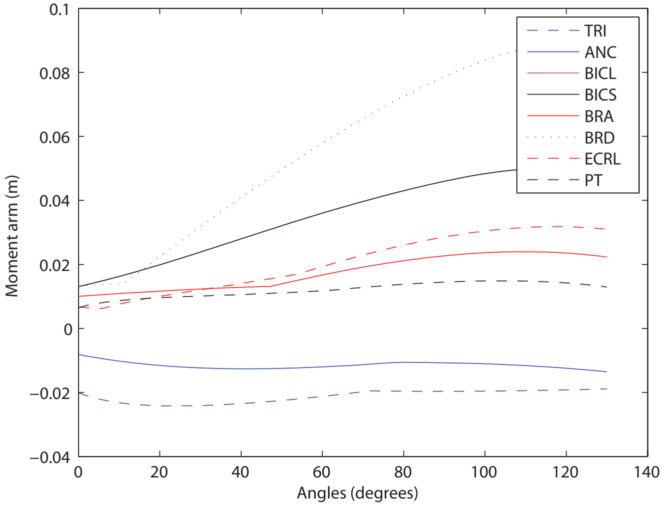

Figure 4.3: Elbow moment arm variation

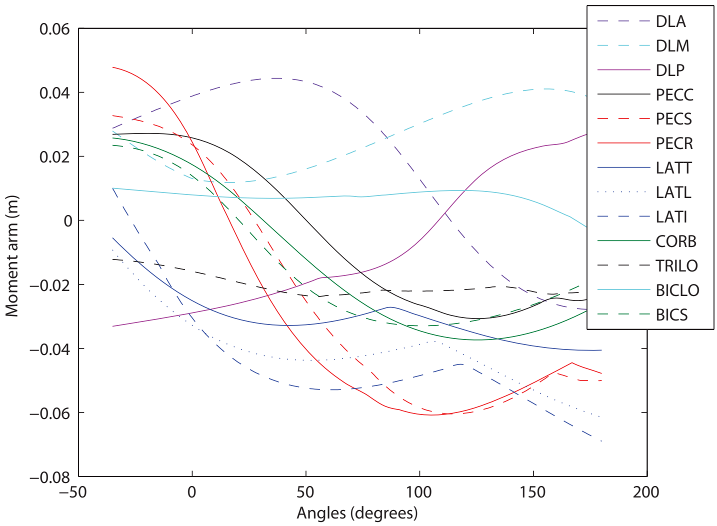

Figure 4.4: Shoulder moment arm variation

the cadavers used for muscle architecture experiments usually are. This statement was neglected in this study. For the numerical examples a specific tension of 330 kPa was used, referring to Garner and Pandy [31], where they developed a general method for estimating upper limb architectural properties in-vivo.

Table 4.1: Upper limb muscle properties used in Paper 1. Moment arms, PCSA and were obtained from Holzbaur et al. (2005).

Muscles	Abbreviation	Function	PCSA (10^{-4}m^2)
Deltoid Posterior	DLP	Extension	1.9
Deltoid Anterior	DLA	Flexion	8.2
Deltoid Middle	DLM	Flexion	8.2
Pectoralis Major Clavicular	PECC	Flexion	2.6
Pectoralis Major Sternal	PECS	Flexion	3.7
Pectoralis Major Ribs	PECR	Flexion	2.8
Latissimus dorsi Thoracic	LATT	Extension	2.8
Latissimus dorsi Lumbar	LATL	Extension	2.8
Latissimus dorsi Iliac	LATI	Extension	2.0
Coracobrachialis	CORB	Flexion	1.7
Triceps Long	TRILO	Extension	5.7
Triceps Lateral	TRILA	Extension	4.5
Triceps Medial	TRIM	Extension	4.5
Anconeus	ANC	Extension	2.5
Biceps Long	BICL	Flexion	4.5
Biceps Short	BICS	Flexion	3.1
Brachialis	BRA	Flexion	7.1
Brachioradialis	BRD	Flexion	1.9
Extensor carpi radialis longus	ECRL	Flexion	2.2
Pronator teres	PT	Flexion	4.0

4.2 Paper 2

Muscle function during gait is usually described in a clinical setting as ‘on’ or ‘off’. To study the forces of the ankle and knee musculature during gait, the numerical method developed in Paper 1 was used. A primary study on static optimization in gait was also presented at the European Society of Movement Analysis for Adults and Children (ESMAC) conference in 2005; conference proceedings are published in Gait and Posture volume 22.

The objective of this study was to evaluate person specific muscle forces during gait and to find a possible way to validate these findings. Together with the Motoriklab at Karolinska University Hospital, gait analysis was executed with simultaneous surface EMG on one subject. An EMG-to-force method was adopted for the study, which is a way to scale and translate EMG data to force units. The method of EMG-to-force provides an opportunity to compare calculated results with a method to estimate in-vivo forces on the individual subject. Evaluated optimal forces from the lower limb model in gait were compared to estimated forces from the EMG-to-force method. Additional comparison to published EMG activation data was performed.

4.2.1 Model description

The lower limb was modelled as a three link-segment (Figures 4.5 and 4.6), including hip, knee and ankle together with 43 musculotendon actuators. Data from gait analysis was exported to SIMM where moment arms were evaluated using ‘the partial velocity’ method [39].

In the primary study presented at ESMAC, the moment arms were based on a set of polynomial fitted expressions described by Menegaldo et al. [47]. These were validated against the musculoskeletal lower limb model described by Delp et al. in 1990 with good correlation. This method of modelling moment arms is a good option if no musculoskeletal software is available.

The PCSA values used in the lower limb model are based on maximal isometric force evaluated in SIMM, which were collected from the literature (Table 4.2) [11, 26, 62]. The value of the specific tension used to derive the PCSA was arbitrary chosen 100 kPa [14], because the value do not influence the result from the optimization. This value will be important if the loading capacity of the system is to be evaluated.

In the evaluation of muscle forces during gait, the cycle is seen as a set of static positions where the forces were evaluated. The chosen performance criterion was the sum of stresses squared. The second power was motivated by results in Paper 1 showing small differences in the evaluated forces due to various powers in the performance functions. Using stresses in the performance criterion the forces are minimized relative to the PCSA, compared to a force-based criterion which tend to provide force relative to the moment arms.

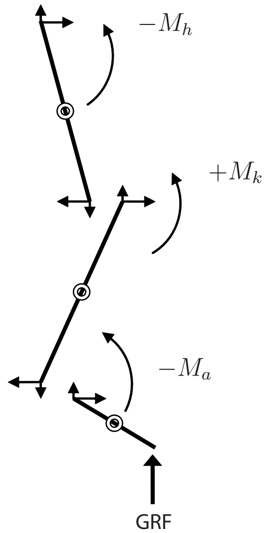

Figure 4.5: Lower limb, free-body diagram with the definition of positive directions of moments in the respective joint, hip joint,M_h, knee joint, M_k, and ankle joint, M_a, according to the gait model (Plug-In-Gait, Vicon Peak, Oxford, UK) used in the motion analysis system (Vicon Peak, Oxford, UK). The ground reaction force was placed arbitrarily.

Figure 4.6: Lower limb, image from SIMM [20], model developed by Delp et al. [21]

Table 4.2: Lower Extremity muscle data. Maximum isometric force were obtained from Delp et al. (1990). Muscles used in the EMG test are marked *. Muscular functions abbreviations; F for flexion, Ex for extension, Add for adduction and Abd for abduction.

Muscles	Abbreviation	Peak Force (N)	Major Function
Gluteus Medius 1	GMED1	546	Hip Abd.
Gluteus Medius 2	GMED2	382	Hip Abd.
Gluteus Medius 3	GMED3	435	Hip Abd.
Gluteus minimus 1	GMIN1	180	Hip Abd.
Gluteus minimus 2	GMIN2	190	Hip Abd.
Gluteus minimus 3	GMIN3	215	Hip Abd.
Semimembranosus	SEMIM	1030	Hip E., Knee F.
Semitendinosus*	SEMIT	328	Hip E., Knee F.
Biceps Femoris Long Head*	BIFEM	717	Hip E., Knee F.
Biceps Femoris Short Head	BICFEMS	402	Hip E., Knee F.
Sartorius	SART	104	Hip & Knee F.
Adductor longus	ADDL	418	Hip Add, F.
Adductor brevis	ADDB	286	Hip Add, F.
Adductor magnus 1	AMAG1	346	Hip Add, F.
Adductor magnus 2	AMAG2	312	Hip Add, F.
Adductor magnus 3	AMAG3	444	Hip Add, F.
Tensor fascia latae	TFL	155	Hip F.
Pectineus	PECT	177	Hip Add., F.
Gracilis	GRA	108	Hip Add., F.
Gluteus maximus 1	GMAX1	382	Hip E., Ex. Rot
Gluteus maximus 2	GMAX2	546	Hip E., Ex. Rot
Gluteus maximus 3	GMAX3	368	Hip E., Ex. Rot
Iliacus	ILIA	429	Hip F., Ex. Rot
Psoas	PSOA	371	Hip F., Ex. Rot
Quadratus femoris	QFEM	254	Hip Ex. Rot.
Inferior gemellus	GEM	109	Ex. Rot.
Piriiormis	PIRI	296	Ex. Rot.
Rectus Femoris*	RECF	779	Hip F., Knee E.
Vastus Medialis*	VASM	1294	Knee E.
Vastus Intermedius	VASI	1365	Knee E.
Vastus Lateralis*	VASL	1871	Knee E.
Gastrocnemius Medialis*	GASM	1113	DorsiF
Gastrocnemius Lateralis*	GASL	488	DorsiF
Soleus*	SOL	2839	DorsiF
Tibialis posterior	TIBP	1270	DorsiF
Flexor digitorum	FDIG	310	PlantarF
Flexor hallucis long	FHALL	322	PlantarF
Tibialis Anterior*	TIBA	603	PlantarF
Peroneus Brevis	PBR	348	PlantarF
Peroneus Longus	PLO	754	PlantarF
Peroneus Tertius	PT	108	DorsiF
Extensor digitorum	EXD	90	DorsiF
Extensor hallucis	EXH	341	DorsiF

Chapter 5

Conclusions and Future work

5.1 Concluding Remarks

The aim of these studies has been to develop a numerical model able to calculate and evaluate individual muscular forces in human postures and movement. A static optimization algorithm was developed and used in two examples, the upper and lower limb, to evaluate muscular forces. The numerical algorithm was time efficient, and no numerical problems has been found in the used problem settings. The algorithm was found easy to modify after purpose of study: small single joint systems with only a few muscles up to large systems with multiple joints with a full set of muscles. It was shown that optimization can reasonably well predict individual muscular forces, but that the accuracy of evaluated forces is dependent of the correctness of the muscular architectural properties. A challenge is to find tools for measuring in-vivo musculoskeletal architectural properties.

One study was based on modelling a simplified system of the upper limb, including the shoulder and elbow joints. By modelling the system with only eight muscles load-sharing and loading properties on the individual muscle contributions can be illustrated, as functions of the model, but also of the criterion chosen. A more complete model, containing 20 muscles, allowed the loading capacity of the system to be evaluated.

In modelling the lower limb in gait, optimal forces were evaluated. Optimization techniques in a numerical setting were proven easy to use together with a motion analysis system. Optimal muscular forces were compared to EMG data. Both individual EMG data and published average EMG data were used. As both the inverse dynamic analysis and the EMG measurements contained uncertainties, the agreement was mediocre. The optimized force variations better matched published average EMG data from gait experiments. On an individual basis, optimization may arguably be more useful in calculating muscle forces.

5.2 Future Perspective

Joining optimization techniques and gait analysis provides an opportunity to evaluate optimal individual muscular forces in pathological gait. In pathologies such as cerebral palsy and rheumatoid arthritis, spasticity, muscular weakness, pain and skeletal dysfunction cause deviations in the gait pattern [13, 29, 51]. Force profiles of the individual muscles can provide an opportunity to better understand the biomechanical cause or consequences of pathological gait patterns and to identify the muscle's function during gait [4, 32].

Gait disturbance is a problem affecting the quality of life for patients with rheumatoid arthritis. Treatment aims at restoring function in the musculoskeletal system. Evaluation of treatment is usually based on subjective assessment [13]. An improved biomechanical analysis of a patient's situations before and after treatment is believed to give a better evaluation of the effect of treatment.

The musculoskeletal models used are based on normal geometry. Deformities in the joints are typical syndromes in patients with, for instance, cerebral palsy and rheumatoid arthritis. These bone or joint deformities can have large negative mechanical effects on the muscle function, resulting in reduced joint moments. 'Lever arm dysfunction' describes a set of conditions in which muscles moment arms become distorted due to bony deformities [29]. A mathematic model which can represent bone deformities must also be identified for more accurate result.

Large challenges are in how to model pathological movement and what properties will be the most important to include in an optimization algorithm to evaluate individual muscular forces. The properties of the performance criterion can be different from that of normal gait under the pathological conditions, and in particular the kinematic and kinetic constraints can affect the optimal situations. It is usually assumed that a performance criterion is related to minimize some physiological cost. This cost in optimization of muscular forces in normal gait is assumed to aim at optimal energy conservation. In connection with pathologies, this minimization is often severely restricted by the constraints. A new way to formulate the performance function is therefore needed. Also, including a variable fiber length, which is a major determinant of muscle strength, in the performance function may be of great importance. Methods to represent pathological muscle function by other values than minimum and maximum forces are an interesting possibility.

Mathematical models are usually dependent on the muscle's architectural properties, such as PCSA. Those values probably differ in pathological muscles. MRI techniques show good possibilities to determine PCSA [5, 48]. A study of the effects on these architectural properties from different pathologies would lead to improved insight into what effect the variation in the muscle's architectural properties have on optimization results.

Bibliography

[1] An, K. N., Kwak, B., Chao, E., and Morrey, B. Determination of muscular force and joint torque–a new technique to solve the indeterminate problem. *Journal of Biomechanical Engineering and Transactions of the ASME 106* (1984), 364–367.

[2] Anderson, F. C., and Pandy, M. G. Static and dynamic optimization solution for gait are practically equivalent. *Journal of Biomechanics 34* (2001), 153–161.

[3] Anderson, F. C., and Pandy, M. G. Individual muscle contributions to support in normal walking. *Gait and Posture 17* (2002), 159–169.

[4] Arnold, A. S., Anderson, F. C., Pandy, M. G., and Delp, S. L. Muscular contributions to hip and knee extension during the single limb stance phase of normal gait: a framework for investigating the causes of crouch gait. *Journal of Biomechanics 38* (2005), 2181–2189.

[5] Arnold, A. S., Salinas, S., Askawa, D. J., and Delp, S. L. Accurancy of muscle moment arms estimated from MRI-based musculoskeletal models of the lower extremity. *Computer Aided Surgery 5* (2000), 108–119.

[6] Bertsekas, D. P. *Constrained Optimization and Lagrange Multipliers Method*. Academic Press, London, UK, 1982.

[7] Blemker, S. S., and Delp, S. L. Three-dimensional representation of complex muscle architectures and geometries. *Annals of Biomedical Engineering 33* (2005), 661–673.

[8] Bogey, R. A., Perry, J., Bontranger, E. L., and Gronley, J. K. Comparison of across-subject EMG profiles using surface and multiple indwelling wire electrodes during gait. *Journal of Electromyography and Kinesiology 10* (2000), 255–259.

[9] Bogey, R. A., Perry, J., and Gitter, A. J. An EMG-to-force processing approach for determining ankle muscle forcs during normal human gait. *IEEE Transactions on Neural Systems and Rehabilitation Engineering 13* (2005), 302–310.

[10] Bojsen-Møller, F. *Rörelse-apparatens anatomi*. Liber AB, Stockholm, Sweden, 2000.

[11] Brand, R. A., Pedersen, D. R., and Friederich, J. A. The sensitivity of muscle force predictions to changes in physiological cross-sectional area. *Journal of Biomechanics 19* (1986), 589–596.

[12] Braune, W., and Fischer, O. *The Human Gait.* Springer, Berlin, Germany, 1987.

[13] Broström, E. *Juvenile idiopathic arthritis— Disease consequences and treatment effects on muscle strength, gait and pain.* PhD thesis, Department of Woman and Child Health, Karolinska Institute, Stockholm, Sweden, 2004.

[14] Buchannan, T. S. Evidence that maximum muscle stress is not a constant: differences in specific tension in elbow flexors and extensors. *Medical Engineering and Physics 17* (1995), 529–53663.

[15] Chadwick, E., and Nicol, A. Elbow and wrist joint contact forces during occupational pick and place activities. *Journal of Biomechanics 33* (2000), 591–600.

[16] Collins, J. J. The redundant nature of locomotor optimization laws. *Journal of Biomechanics 28* (1995), 251–267.

[17] Crowninshield, R. D., and Brand, R. A. A physiologically based criterion of muscle force prediction in locomotion. *Journal of Biomechanics 14* (1981), 793–801.

[18] Davis, J., Kaufman, K., and Lieber, R. Correlation between active and passive isometric force and intra muscular pressure in the isolated rabbit tibialis anterior muscle. *Journal of Biomechanics 36* (2003), 505–512.

[19] De Luca, C. The use of surface electromyography in biomechanics. *Journal of Applied Biomechanics 13* (1997), 135–163.

[20] Delp, S. L., and Loan, J. P. A graphic-based software system to develop and analyze models of musculoskeletal structures. *Computers in Biology and Medicine 25* (1995), 21–34.

[21] Delp, S. L., Loan, J. P., Hoy, M. G., Zajac, F. E., Topp, E. L., and Rosen, J. M. An interactiv graphic-based model of the lower extremity to study orthopedic surgical procedures. *IEEE Transactions on Biomedical Engineering 37* (1990), 757–767.

[22] Dul, J., Townsend, M., Shavi, R., and Johnsson, G. Muscular synergism— I. On criteria for load sharing between synergistic muscles. *Journal of Biomechanics 17* (1984), 663–673.

[23] Farewik, M. Strength measurement apparatus for the lower extremities. Master's thesis, Royal Institute of Technology, Stockholm, Sweden, 2005.

[24] Forster, E., Simon, U., Augat, P., and Claes, L. Extension of a state-of-the-art optimization criterion to predict co-contraction. *Journal of Biomechanics 37* (2004), 577–581.

[25] Fridén, J., and Lieber, R. L. Quantitative evaluation of the posterior deltoid to triceps tendon transfer based on muscle architectural properties. *The Journal of Hand Surgery 26A* (2001), 147–155.

[26] Friederich, J. A., and Brand, R. A. Muscle fiber architecture in the human lower limb. *Journal of Biomechanics 23* (1990), 91–95.

[27] Fukunaga, T., Miyatani, M., Tachi, M., Kouzaki, M., Kawakami, Y., and H-Kanehisa. Muscle volume is a major determinant of joint torque in humans. *Acta Physiologica Scandinavica 172* (2002), 249–255.

[28] Fukunaga, T., Roy, R., Shellock, F., Hodgson, J., Day, M., Lee, P., Kwong-Fu, H., and Edgerton, V. Physiological cross-sectional area of human leg muscles based on magnetic resonance imaging. *Journal of Orthopaedic Research 10* (1992), 926–934.

[29] Gage, J. R. *The Treatment of Gait Problems in Cerebral Palsy*. Mac Keith Press, London, UK, 2004.

[30] Gage, J. R., Deluca, P. A., and Renshaw, T. S. Gait analysis: Principles and applications. *The American Academy of Orthopedic Surgeons 77-A* (1995), 1607–1623.

[31] Garner, B. A., and Pandy, M. G. Estimation of muscolutendon properties in the human upper limb. *Annals of Biomedical Engineering 31* (2002), 207–220.

[32] Goldberg, S. R., Anderson, F. C., Pandy, M. G., and Delp, S. L. Muscles that influence knee flexion velocity in double support: implications for stiff knee gait. *Journal of Biomechanics 37* (2004), 1189–1196.

[33] Gutierrez, E. M. *Gait Strategy in Myelomeningocele: Movements, Mechanics and Methods*. PhD thesis, Department of Surgical Sciences, Section for Orthopedics, Karolinska Institute, Stockholm, Sweden, 2003.

[34] Happee, R., and Van der Helm, F. The control of shoulder muscles during goal directed movement, an inverse dynamic analysis. *Journal of Biomechanics 28* (1995), 1179–1191.

[35] Hof, A. EMG and muscle force: an introduction. *Human Movement Science 3* (1984), 119–153.

[36] Hof, A., Elzinga, H., Grimmius, W., and Halbertsma, J. Speed dependence of averaged EMG profiles in walking. *Gait and Posture 16* (2002), 78–86.

[37] Hof, A., Elzinga, H., Grimmius, W., and Halbertsma, J. Detection of non-standard EMG profiles in walking. *Gait and Posture 21* (2005), 171–177.

[38] Holzbaur, K. R. S., Murray, W. M., and Delp, S. L. A model of the upper extremity for simulating musculoskeletal surgery and analyzing neuromuscular control. *Annals of Biomedical Engineering 33* (2005), 829–840.

[39] Kane, T., and Levinson, D. *Dynamics: Theory and Applications*. McGraw-Hill, New York, USA, 1985.

[40] Kaufman, K., An, K., Litchy, W., and Chao, E. Physiological prediction of muscle forces— I. Theoretical formulation. *Neuroscience 3* (1991), 781–792.

[41] Kirtley, C. *Clinical Gait Analysis*, first ed. Elsevier, London, UK, 2006.

[42] Kreyszig, E. *Advanced Engineering Mathematics*, eighth ed. Wiley, New York, USA, 1999.

[43] Lieber, R. L. *Skeletal Muscle Structure and Functions: Implications for Physical Therapy and Sports Medicine*. Williams and Wilkins, Baltimore, USA, 1992.

[44] Lieber, R. L., and Fridén, J. Clinical significance of skeletal muscle architecture. *Clinical Orthopaedic and Related Research 383* (2001), 140–151.

[45] Loren, G. J., Shoemaker, S. D., Burkholder, T. J., Jacobsson, M. D., Friden, J., and Lieber, R. L. Human wrist motors: Biomechanical design and application to tendon transfers. *Journal of Biomechanics 29* (1996), 331–342.

[46] McGinnis, P. M. *Biomechanics of sport and exercise.* Human Kinetics, Champaign, USA, 1999.

[47] Menegaldo, L. L., de Toledo Fleury, A., and Weber, H. I. Biomechanical modeling and optimal control of human posture. *Journal of Biomechanics 36* (2003), 1701—1712.

[48] Nakamura, Y. *Advanced Robotics, Redundancy and Optimization.* Addison-Wesley, USA, 1991.

[49] Nigg, B. M., and Herzog, W. *Biomechanics of the Musculo-skeletal System*, second ed. Wiley, West Sussex, England, 1999.

[50] Pedotti, A., Krishnan, V. V., and Stark, L. Optimization of muscle-force sequencing in human locomotion. *Mathematical Bioscience 38* (1978), 57–76.

[51] Perry, J. *Gait Analysis: Normal and Pathological Function.* SLACK, 1992.

[52] Powell, P. L., Roy, R. R., Kanim, P., Bello, M., and Edgerton, V. R. Predictability of skeletal muscle tension from architectural determinations in guinea pig hindlimbs. *Journal of Applied Physiology 57* (1984), 1715–1721.

[53] Praagman, M., Chadwick, E., van der Helm, F., and Veeger, H. The relationship between two different mechanical cost functions and muscle oxygen consumption. *Journal of Biomechanics 39* (2006), 758–765.

[54] Raikova, R. T. A model of the flexion-extension motion in the elbow joint-some problems concerning muscle forces modelling and computation. *Journal of Biomechanics 29* (1996), 763–772.

[55] Rasmussen, J., Damsgaard, M., and Voigt, M. Muscle recruitment by the min/max criterion — a comparative numerical study. *Journal of Biomechanics 34* (2001), 409–415.

[56] Sacks, R. D., and Roy, R. R. Architecture of the hind limb muscles of cats functional significance. *Journal of Morphology 173* (1982), 185–195.

[57] Seireg, A., and Arvikar, R. J. The prediction of muscular load sharing and joint forces in the lower extremities during walking. *Journal of Biomechanics 8* (1975), 89–102.

[58] Strang, G. *Introduction to Applied Mathematics*. Wellesly-Cambridge Press, Wellesly, MA, USA, 1986.

[59] Strang, G. *Linear Algebra and its Applications*, third ed. Harcourt Brace Jovanovich Collage Publishers, Orlando, Florida, USA, 1988.

[60] Ward, S., and Lieber, R. Density and hydration of fresh and fixed human skeletal muscle. *Journal of Biomechanics 38* (2005), 2317–2320.

[61] White, S. C., and Winter, D. A. Predicting muscle forces in gait from EMG signals and musculotendon kinematics. *Journal of Electromyography and Kinesiology 2* (1993), 217–231.

[62] Wickiewicz, T., Roy, R., Powell, P., and Edgerton, V. Muscle architecture of the human lower-limb. *Clinical Orthopaedics and Related Research 179* (1983), 275–283.

[63] Winter, D. *The biomechanics and motor control of human gait*, third ed. University of Waterloo Press, Waterloo, Canada, 2005.

[64] Yamaguchi, G. T., Moran, D. W., and Si, J. A computationally efficient method for solving the redundant problem in biomechanics. *Journal of Biomechanics 28* (1995), 999–1005.

[65] Zajac, F. E. Mucsle and tendon: Properties, models, scaling, and application to biomechanics and motor control. *Critical Reviews in Biomedical Engineering 17* (1989), 359–411.

[66] Zajac, F. E., and Gordon, M. Determining muscle function and action in multi-articular movement. *Exercise and Sport Science Reviews 17* (1989), 187–230.

[67] Zajac, F. E., Neptune, R. R., and Kautz, S. A. Biomechanics and muscle coordination of human walking, part I: Introduction to concepts, power transfer, dynamics and simulations. *Gait and Posture 16* (2002), 215–232.

[68] Zatsiorsky, V. M. *Kinematics of Human Motion*, first ed. Human Kinetics, Champaign, USA, 1998.

[69] Zatsiorsky, V. M. *Kinetics of Human Motion*, first ed. Human Kinetics, Champaign, USA, 2002.

Paper 1

1